ACS Chemical Neuroscience

Research Article

pubs.acs.org/chemneuro

p53 Functional Inhibitors Behaving Like Pifithrin-β Counteract the Alzheimer Peptide Non-β-amyloid Component Effects in Human SH-SY5Y Cells

Eleonora Da Pozzo,[†] Valeria La Pietra,[‡] Barbara Cosimelli,[‡] Federico Da Settimo,[†] Chiara Giacomelli,[†] Luciana Marinelli,[‡] Claudia Martini,*[,†] Ettore Novellino,[‡] Sabrina Taliani,[†] and Giovanni Greco[‡]

[†]Dipartimento di Farmacia, Università di Pisa, Via Bonanno Pisano 6, 56126 Pisa, Italy

[‡]Dipartimento di Farmacia, Università di Napoli "Federico II", Via Domenico Montesano 49, 80131 Naples, Italy

Supporting Information

ABSTRACT: Alzheimer's disease (AD) develops from a complex setting of genetic and biochemical alterations, including an increased level of p53 in the brain. Here, the robust and specific activation of p53 by the fibrillar non-β-amyloid component (NAC) of AD was demonstrated in human neuroblastoma SH-SY5Y cells. For the first time, the increase in the level of p53 target gene transcription, the cell cycle arrest, and the induction of apoptosis elicited by NAC were evidenced. These effects were counterbalanced by pifithrin-β, a small molecule interfering with the p53 functions. Using the structure of a pifithrin-β analogue as a reference, a pharmacophore-based virtual screening of the ZINC database was performed. Among the resulting hits, 20 druglike heterocyclic compounds were selected and evaluated for their neuroprotective activity against fibrillar NAC in the human SH-SY5Y cellular model. Three compounds exhibited neuroprotective effects. In particular, 2-(4-methoxyphenyl)-7-methyl-7*H*-pyrazolo[4,3-*e*][1,2,4]triazolo[1,5-*c*]pyrimidine resulted in a promising lead compound for further development of anti-AD agents in terms of neuroprotection, reducing the rate of NAC-induced cell death with an activity higher than that of pifithrin-β, as a result of a more effective functional inhibition of p53 target gene transcription.

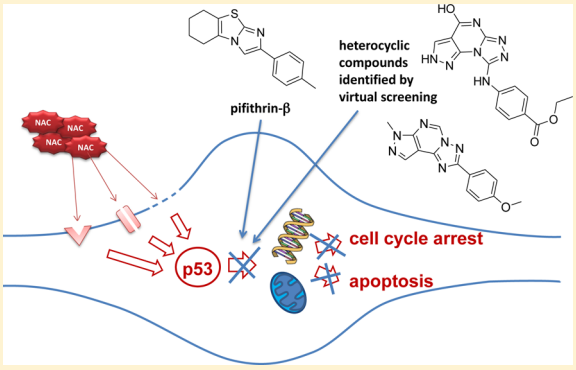

KEYWORDS: *p53, Alzheimer's disease, pifithrin-β, non-β-amyloid component (NAC), virtual screening, database searching*

The pathogenesis of Alzheimer's disease (AD) develops from a complex mix of genetic and biochemical factors, including an increased level of production of synuclein proteins (such as β-amyloid) and significant alterations in cell signaling systems.[1,2] In particular, the p53 intracellular pathway seems to be involved, as revealed by the increased levels of p53 evidenced in brains of AD patients.[3,4] This finding could be one of the reasons for the massive neuronal death occurring during the disease. Indeed, p53 plays key roles in the regulation of cell viability by stimulating specific gene expression (p21, Bax, and PUMA) and interacting with mitochondrial proteins, to arrest the cell cycle and/or to activate programmed cell death.[5,6] Interestingly, apoptosis in AD microglia and in β-amyloid-expressing neurons was found to be mediated by p53,[7,8] and an increase in the level of p53 transcription was associated with neuron β-amyloid deposition.[9] Nevertheless, β-amyloid is not the only active factor responsible for neurotoxicity in AD. A small peptide, the non-β-amyloid component (NAC), is the second major constituent of plaques in AD brains and is closely colocalized with β-amyloid.[10] NAC is more abundant in the center portion of the amyloid plaque rather than in the periphery; this peculiar distribution suggests that NAC might promote β-amyloid aggregation,[11,12] thus playing a role in the early phase of AD pathogenesis. Although NAC neurotoxicity has already been reported in the literature,[13,14] little is known about the cellular pathway activated by this toxic protein. Previous studies performed on rat pheochromocytoma cells showed that NAC treatment caused an increase in p53 levels.[15] The p53 functional inhibitor pifithrin-α[16] (Chart 1) is a small molecule reported to behave like an antiapoptotic agent in neurodegenerative models.[8,17−19] Pifithrin-α is a prodrug that under physiological conditions spontaneously undergoes ring closure to yield pifithrin-β[20] [**1** (Chart 1)]. In light of these findings, previous studies have been devoted to identifying druglike compounds endowed with pharmacological activities better than those exhibited by pifithrin-α and pifithrin-β.[21−23]

The primary aim of this study was to evaluate the involvement of p53 signaling in human neuroblastoma SH-SY5Y cells,[13] a cell line suitable for AD models,[24] treated with

Received: December 9, 2013
Revised: February 24, 2014
Published: March 19, 2014

 © 2014 American Chemical Society dx.doi.org/10.1021/cn4002208 | *ACS Chem. Neurosci.* 2014, 5, 390−399

Chart 1. Structures of Pifithrin-α and Pifithrin-β (1)

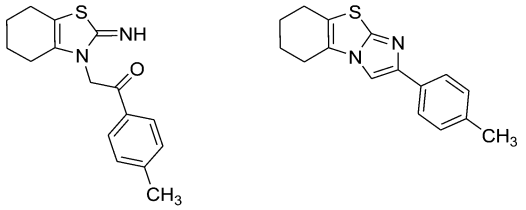

pifithrin-α pifithrin-β (**1**)

NAC as a toxic insult. Subsequently, to set up an *in vitro* predictive test for the assessment of potential anti-AD agents that can interfere with p53 function, the NAC effects were evaluated in the presence of pifithrin-β. Given the great demand for effective anti-AD compound agents, the second goal of our research was the identification of new antineurodegenerative compounds. A database search was performed to identify a small number of commercially available druglike compounds, structurally related to pifithrin-β. Finally, the AD cellular model previously validated using pifithrin-β was employed to evaluate the selected compounds for their neuroprotective activity against NAC.

RESULTS AND DISCUSSION

NAC Cell Treatment. Protein conformation-dependent neurotoxicity is a significant theme in AD.[25] The amyloid cascade hypothesis suggests that the β-amyloid fibrillar form plays a primary pathogenic role in AD. Recent evidence suggests a more complex mechanism, as neurotoxicity may also be exerted by rather small soluble aggregates, including oligomers.[26,27]

The neurotoxicity of NAC treatment is well-established, as described in several papers on cellular and animal models;[13−15,28−33] however, the molecular mechanism responsible for the toxicity exerted by NAC remains largely elusive, and it is still not clear whether the most deleterious peptide state is represented by the fibrillar or the nonfibrillar form. In this vein, we decided to proceed by investigating the neurotoxicity of NAC in both peptide forms (nonfibrillar and fibrillar states), as previously tested in different experimental settings.[13,15,30]

As the NAC fragments are able to form β-sheet and amyloid-like filaments,[13] the NAC neurotoxic effect was evaluated with its nonfibrillar and fibrillar forms (as described in Cell Model Characterization). SH-SY5Y cells were treated with aggregated and nonaggregated NAC at different concentrations (1−50 μM) for 24 h, and cell viability was assessed.

According to previously published data,[13] the effects elicited by NAC on cell viability strictly depend on the peptide aggregation state (Figure 1). In particular, treatment with nonfibrillar NAC produced a moderate decrease in cell viability at a concentration of only 50 μM (82.50 ± 3.50%; $p < 0.05$). Conversely, fibrillar NAC elicited an efficient and dose-dependent toxic insult in human SH-SY5Y cells, significantly reducing cell viability at concentrations of 10 and 50 μM (63.29 ± 2.14 and 21.33 ± 5.81%, respectively; $p < 0.001$). On the basis of these data, the aggregated (fibrillar) NAC at a concentration of 10 μM proved to represent an efficient toxic insult in human SH-SY5Y cells and therefore was used for the subsequent experiments.

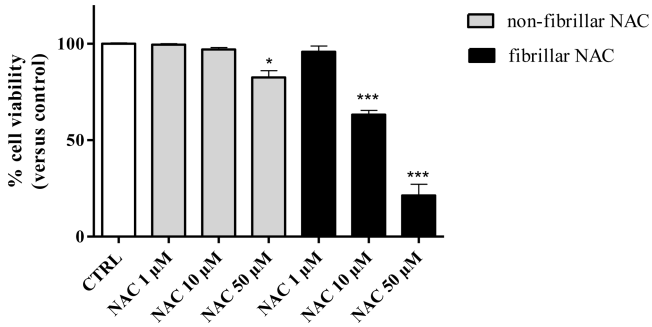

Figure 1. Different aggregating states and concentrations of NAC affected cell viability. SH-SY5Y cells were exposed for 24 h to increasing concentrations of NAC (1−50 μM) in the nonfibrillar or fibrillar aggregation state. The data are expressed as the mean percentage of cell viability vs the control (DMSO), which was set to 100%. Values represent the means ± SEM of at least five independent experiments. *$p < 0.05$ and ***$p < 0.001$ vs the control.

Evaluation of p53 Signaling following the NAC Treatment of Cells in the Absence or Presence of the Functional p53 Interfering Agent, Pifithrin-β. *Transcription of p53 Target Genes.* It is well-known that p53 activates specific proapoptotic genes (p21, Bax, PUMA, and MDM2) to promote the arrest of the cell cycle and the mitochondrial permeability transition. To test whether the toxic effect of NAC in human SH-SY5Y cells derived from the activation of p53 pathways, the relative mRNA quantification of p53 target genes was performed by means of real-time RT-PCR. Notably, in cells exposed to 10 μM fibrillar NAC, significant increases in the levels of transcription of p53 target genes such as MDM2, p21, and BAX ($p < 0.01$, $p < 0.001$, and $p < 0.001$, respectively) were detected (Figure 2). Additionally,

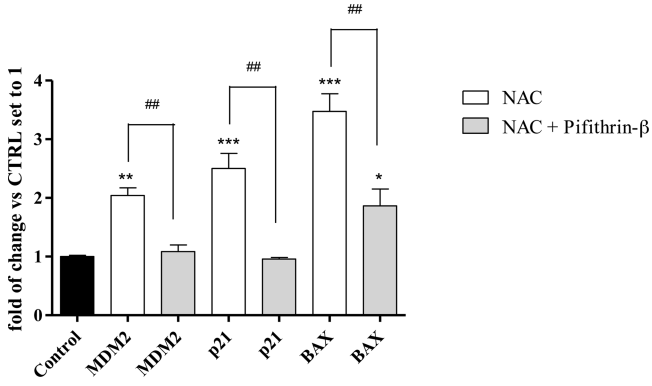

Figure 2. NAC increased the level of p53 target gene transcription. The relative quantification of MDM2, p21, and BAX mRNA was performed by real-time RT-PCR. SH-SY5Y cells were treated for 24 h with 10 μM fibrillar NAC in the absence or presence of 10 μM pifithrin-β. The data are expressed as the mRNA fold increase vs the control, which was set to 1. Values represent the means ± SEM of at least three independent experiments. *$p < 0.05$, **$p < 0.01$, and ***$p < 0.001$ vs the control.

SH-SY5Y cells were pre-exposed for 3 h to 10 μM pifithrin-β, and then 10 μM NAC was added for 24 h. Interestingly, the pifithrin-β pretreatment preserved the increase in mRNA levels of p53 target genes ($p < 0.01$ with respect to mRNA levels of not pretreated cells), with the only exception being BAX mRNA levels that remained significantly higher with respect to the control ($p < 0.05$) (Figure 2). These data support the suggestion that the NAC neurotoxicity in human SH-SY5Y cells involves the activation of p53 pathways. This is confirmed by the almost complete abrogation of the NAC-induced gene

dx.doi.org/10.1021/cn4002208 | ACS Chem. Neurosci. 2014, 5, 390−399

transcriptional increase that occurs in cells pre-exposed to the functional p53 inhibitor pifithrin-β.

Evaluation of Cell Cycle Arrest. One of the pivotal consequences of p53 activation, due to the transcription of cyclin-dependent kinase inhibitor p21, is the cell cycle arrest at the G1 or G2/M phase. For this reason, the cell cycle analyses were performed on SH-SY5Y cells exposed to 10 μM NAC and 10 μM pifithrin-β, alone or in combination.

In accordance with the transcription data, the investigation of the cell cycle after exposure for 24 h to NAC revealed an arrest in the G2 phase, as demonstrated by the significant increase in the number of cells in the G2/M phase and the related reduction in the number of cells in the G1 phase (Figure 3).

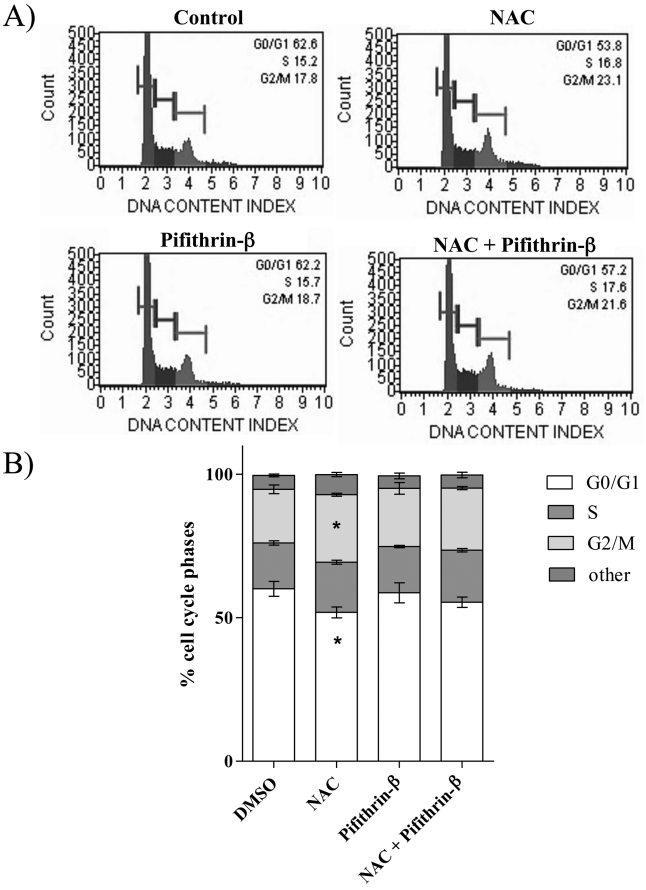

Figure 3. NAC treatment induced cell cycle arrest. SH-SY5Y cells were treated for 24 h with DMSO, with 10 μM pifithrin-β, and with 10 μM fibrillar NAC, with or without being pre-exposed to 10 μM pifithrin-β. (A) Representative DNA content profile of DMSO-treated (control) and drug-treated cells. (B) Bar chart showing the percentage of SH-SY5Y cells in G1, S, and G2/M phases. The data represent the means ± SEM of at least three independent experiments. *$p < 0.05$ vs the control.

Conversely, pifithrin-β treatment did not induce any perturbation in the cell cycle. Interestingly, pre-exposure to pifithrin-β prevented the NAC-induced cell cycle arrest, demonstrating that the functional inhibition of p53 counteracted the effects of NAC on the cell cycle (Figure 3). These findings clearly suggest that NAC and pifithrin-β take part in p53 signaling to regulate the cell cycle, as supported by the increase in the level of cycline kinase inhibitor p21 transcription in cells exposed to NAC (Figure 2), and by the alteration in the cell distribution profile among the cell cycle phases (Figure 3).[34] Nevertheless, other p53-independent mechanisms cannot be excluded.

Evaluation of Apoptosis. As one of the p53 functions is activation of programmed cell death, the ability of NAC to induce apoptosis in SH-SY5Y cells was investigated. The living state of cells exposed to drugs for 24 h was assessed using the Annexin V/Propidium Iodide combined assay, as described in Methods. Treatment with 10 μM fibrillar NAC caused an increase in the apoptotic cell percentage ($p < 0.001$) with respect to the control, whereas incubation with 10 μM pifithrin-β alone did not induce apoptosis. Of note, in cells treated with 10 μM pifithrin-β and NAC, a decrease in the level of apoptosis ($p < 0.01$ vs the control) with respect to cells without pre-exposure ($p < 0.001$ vs the control) was found, even if the decrease in the rate of cell death was not complete (Figure 4). Interestingly, such partial counterbalance by pifithrin-β cell treatment of NAC-induced apoptosis is in accordance with our BAX transcriptional data. In fact, the BAX mRNA level was found to be decreased by the pifithrin-β cell pre-exposure, but it remained significantly higher than the control (Figure 2).

Notably, our primary purpose to set up an *in vitro* model that is reasonably predictive in assessing the pharmacological activity of compounds interfering with p53 signaling was achieved, as confirmed by the results obtained in the experiments described above. Indeed, all data indicated that p53 plays a key role in the NAC-induced neurotoxicity and that a functional inhibitor of p53, such as pifithrin-β, is able to counteract the effects of the NAC toxic insult.

Database Searching To Identify Pifithrin-β-like Compounds To Be Evaluated as Neuroprotective Agents. In spite of many studies focusing on the pifithrin-β molecular mechanism, the exact pharmacological target of this compound has not been identified. Therefore, our search for new chemical entities behaving like pifithrin-β was necessarily restricted to ligand-based methods such as database searching.[35] To date, a certain amount of molecules related to pifithrin-α and pifithrin-β have been investigated.[20−23] In particular, Barchechath et al.[22] reported that aromatic derivatives of pifithrin-β, characterized by an imidazo[2,1-*b*]benzothiazole (IBT) scaffold, possess good cytoprotective properties. These properties were further improved by increasing the lipophilicity of the substituent at the *para* position of the phenyl ring attached to position 2 of the IBT nucleus. One of the best performing IBT derivatives was endowed with a pyrrolidinyl group in such a position (IBT-60, **2** in Figure 5). We took this compound as a reference structure to perform a virtual screening of the "lead-now" subset of commercially available compounds filed in the ZINC database.[36] As a query, the following pharmacophoric features automatically extracted from **2** using the Phase software (Phase, version 3.2, Schrödinger, LLC, New York) were used: four aromatic rings, a hydrogen bond acceptor, and a hydrophobic point (Figure 5).

In the virtual screening analysis, only those structures matching a minimum of four out of six sites and provided with a similarity index ("fitness score" calculated with respect to compound **2**) of >2.0 were retained. The virtual screening returned 187 hits that were first clustered into chemically homogeneous groups and then visually inspected. Twenty compounds were selected, purchased, and biologically evaluated. Table 1 lists the structures of the selected compounds (**3**−**22**) together with their fitness scores, the ZINC codes, and the vendor codes. All the computational details are given in Virtual Screening in Methods.

dx.doi.org/10.1021/cn4002208 | ACS Chem. Neurosci. 2014, 5, 390−399

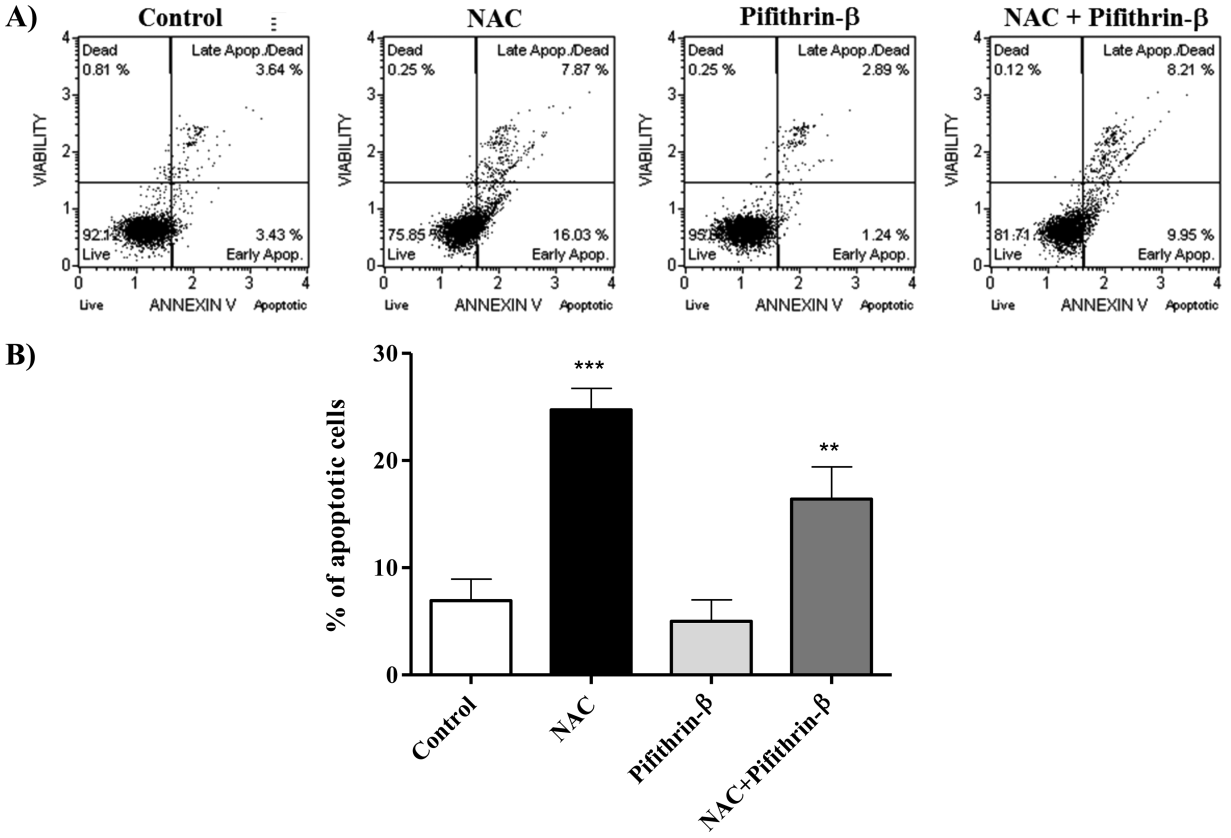

Figure 4. NAC induced apoptotic cell death. SH-SY5Y cells were treated for 24 h with DMSO, with 10 μM pifithrin-β, and with 10 μM fibrillar NAC, with or without being pre-exposed to 10 μM pifithrin-β. (A) Representative apoptosis profiles of DMSO-treated (control) and drug-treated cells. (B) Bar chart showing the percentage of apoptotic cells. The data represent the means ± SEM of at least three independent experiments. $^{**}p <$ 0.01 and $^{***}p < 0.001$ vs the control.

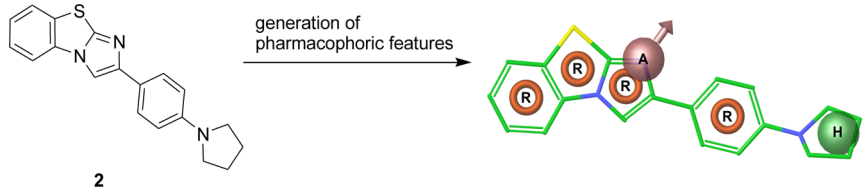

2

Figure 5. Pharmacophoric features extracted from compound **2**:[22] a hydrogen bond acceptor (A), four aromatic rings (R), and a hydrophobic point (H).

The structures of the purchased compounds were confirmed by ^{1}H nuclear magnetic resonance (NMR) spectra and elemental analysis (Supporting Information). The solubility of each compound under the experimental conditions (cell culturing complete medium with 1% DMSO) was estimated as reported in Assessment of Compound Solubility in Cell Experimental Buffer. Compounds **6**, **13**, **15**, **16**, **18**, and **21** could not be tested because they were insufficiently soluble. Poor aqueous solubility is a serious drawback when dealing with druglike molecules rather than with real drugs; this problem cannot be circumvented because of the lack of experimental or reliable calculated values of aqueous solubility for most of the compounds filed in the currently employed databases.[38]

Cytotoxicity of Selected Heterocyclic Compounds. The evaluation of the selected small molecules as potential anti-AD agents was performed by means of the pharmacological predictive *in vitro* model set up in this study. As mentioned, six of the 20 selected heterocyclic compounds were very weakly soluble in cell experimental buffer; thus, we focused our attention on the 14 remaining compounds (**3**−**5**, **7**−**12**, **14**, **17**, **19**, **20**, and **22**), endowed with sufficient aqueous solubility. These compounds and pifithrin-β were evaluated first for their cytotoxicity.

SH-SY5Y cells were treated for 24 h with each compound at concentrations of 1 and 10 μM. The results indicated that none of them was cytotoxic at 1 μM (Figure 6A). The cytotoxicity assay performed at a compound concentration of 10 μM, as reported in Figure 6B, showed that **4**, **12**, and **19**, together with pifithrin-β, did not affect the cell survival with respect to the control. Compound **3** was shown to be very weakly soluble in cell experimental buffer at 10 μM, and therefore, it was not considered for this cytotoxic experiment.

Neuroprotective Activities of Selected Heterocyclic Compounds. The noncytotoxic compounds (**4**, **12**, and **19**) were subsequently tested to assess their neuroprotective activity in the NAC-based cell model. Pifithrin-β was used as the reference standard compound. The assay was performed by

dx.doi.org/10.1021/cn4002208 | ACS Chem. Neurosci. 2014, 5, 390−399

Table 1. Structures, Fitness Scores,[a] ZINC Codes, and Vendor Codes of the Compounds Selected for Evaluation as Novel Neuroprotective Agents

Compound	Structure	Fitness score	ZINC code	Vendor code
3	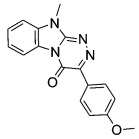	2.192	ZINC01647486	synthesized as in ref. 37
4	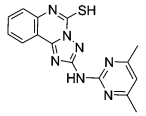	2.053	ZINC12390525	Amb1980174
5	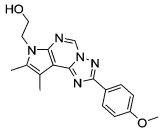	2.370	ZINC06661308	Amb798385
6	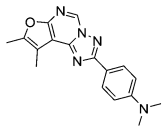	2.550	ZINC05304894	Amb784281
7	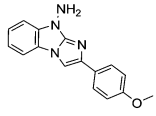	2.461	ZINC00444962	Amb8568721
8	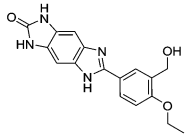	2.255	ZINC67966365	Amb13947555
9	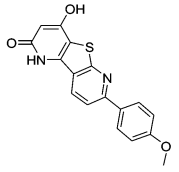	2.225	ZINC05817928	Amb10229623
10	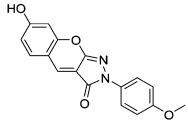	2.173	ZINC33020966	Amb16431857
11	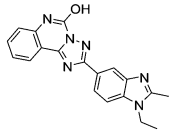	2.623	ZINC08156627	Amb105870
12	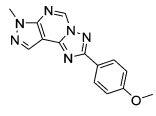	2.425	ZINC00463219	Amb1065628

Compound	Structure	Fitness score	ZINC code	Vendor code
13	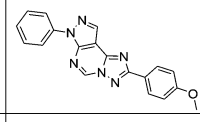	2.302	ZINC00206090	Amb1074860
14	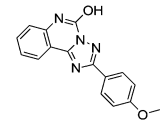	2.400	ZINC08685750	Amb1251605
15	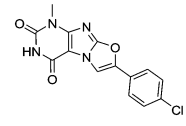	2.330	ZINC00265511	Amb1286577
16	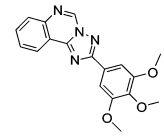	2.356	ZINC05013057	Amb1396845
17	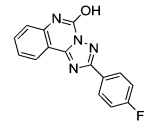	2.162	ZINC09940309	Amb16736327
18	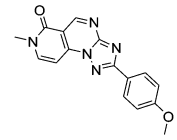	2.417	ZINC12406861	Amb2199629
19	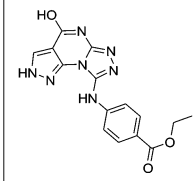	2.030	ZINC35682017	Amb8496038
20	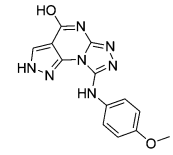	2.231	ZINC35682011	Amb9830443
21	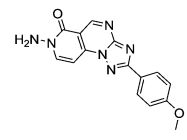	2.417	ZINC13691236	Amb2199953
22	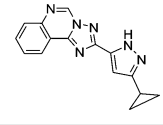	2.345	ZINC05052886	Amb5627760

[a]The fitness score of each compound (ranging from 0 to 3, where 3 is the "best" value) was calculated by taking compound **2**[22] as the reference structure (see Figure 5).

dx.doi.org/10.1021/cn4002208 | ACS Chem. Neurosci. 2014, 5, 390−399

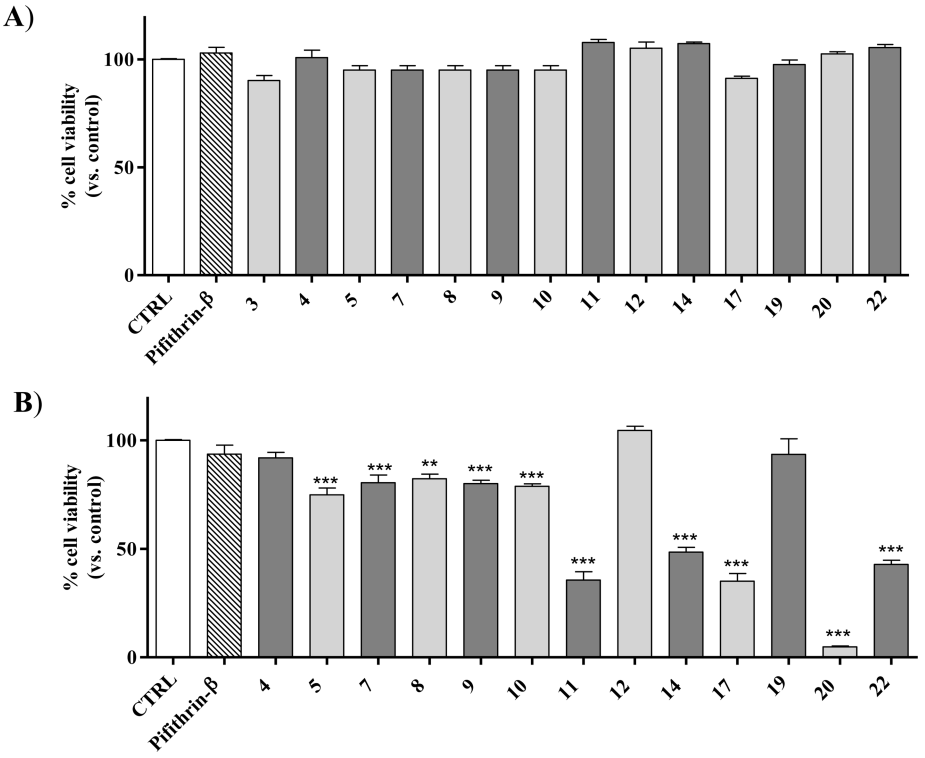

Figure 6. Cytotoxic effects of the tested compounds and pifithrin-β at 1 (A) and 10 μM (B) on SH-SY5Y cells. The data are expressed as mean percentages of cell viability vs the control that was set to 100%. Values represent the means ± SEM of at least five independent experiments. $^{**}p < 0.01$ and $^{***}p < 0.001$ vs the control.

exposing cells first to each compound at concentrations of 1 and 10 μM and then to 10 μM fibrillar NAC. After 24 h, the viability assay showed that the pretreatments with 1 and 10 μM pifithrin-β exerted neuroprotective effects with respect to cells exposed only to NAC ($p < 0.01$) (Figure 7). Notably, **12**, a

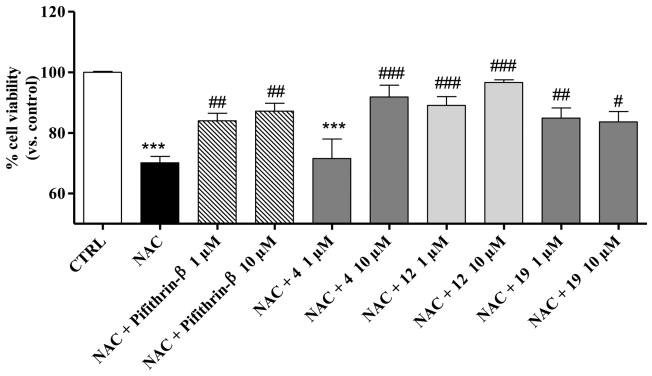

Figure 7. Neuroprotective effects of compounds **4**, **12**, and **19**. SH-SY5Y cells were treated with 10 μM fibrillar NAC in the absence or presence of each tested compound at concentrations of 1 and 10 μM. The data are expressed as the mean percentages of cell viability vs the control, which was set to 100%. Data represent the means ± SEM of at least five independent experiments. $^{***}p < 0.001$ vs the control; $^{\#}p < 0.05$, $^{\#\#}p < 0.01$, and $^{\#\#\#}p < 0.001$ vs 10 μM NAC.

pirazolotriazolopyrimidine derivative, was more effective than pifithrin-β against neuronal death ($p < 0.005$ for both the assessed concentrations). The mean viability of cells pre-exposed to **12** was higher than that of cells pretreated with pifithrin-β (89.06 ± 2.89 and 83.00 ± 2.49%, respectively, at a concentration of 1 μM, and 96.66 ± 0.85 and 87.16 ± 2.64%, respectively, at a concentration of 10 μM). Compound **19** displayed an efficacy similar to that of pifithrin-β (mean cell viability of ~85% for both the tested concentrations), whereas **4** exhibited a strong protective effect with respect to that of pifithrin-β at a concentration of 10 μM; however, **4** it completely lost its neuroprotective activity when used at a concentration of 1 μM.

Investigation of the Neuroprotective Activity of Compound 12. Among the investigated heterocyclic derivatives, **12** exhibited the best neuroprotective activity; thus, further experiments were performed to determine the concentration of **12** capable of inhibiting NAC-induced cell death by 50% (EC_{50}), using pifithrin-β as the reference standard (Figure 8A). Interestingly, the nonlinear regression fitting of the data showed that **12** (mean EC_{50} value of 23.4 nM) was nearly 4 times more effective than pifithrin-β (mean EC_{50} value of 89.1 nM) as a neuroprotective agent.

As described above for cotreatment of cells with NAC and pifithrin-β, the relative mRNA quantification of p53 target genes in SH-SY5Y cells, pre-exposed to 10 μM compound **12** and then supplemented with 10 μM NAC for 24 h, was performed by means of real-time RT-PCR. Remarkably, the compound **12** cell pretreatment, analogous to pifithrin-β pretreatment, preserved the NAC-induced increase in mRNA levels of p53 target genes ($p < 0.01$ for MDM2 and p21 genes and $p < 0.005$ for BAX gene, with respect to mRNA levels of cells not pretreated with compound **12**) (Figure 8B). These data demonstrate that the neuroprotective effect of **12** is mediated by the inhibition of p53, as confirmed by the abrogation of the NAC-induced gene transcriptional increase. Interestingly, **12** seems to be more effective in BAX mRNA inhibition than pifithrin-β, and this behavior may be responsible

dx.doi.org/10.1021/cn4002208 | ACS Chem. Neurosci. 2014, 5, 390−399

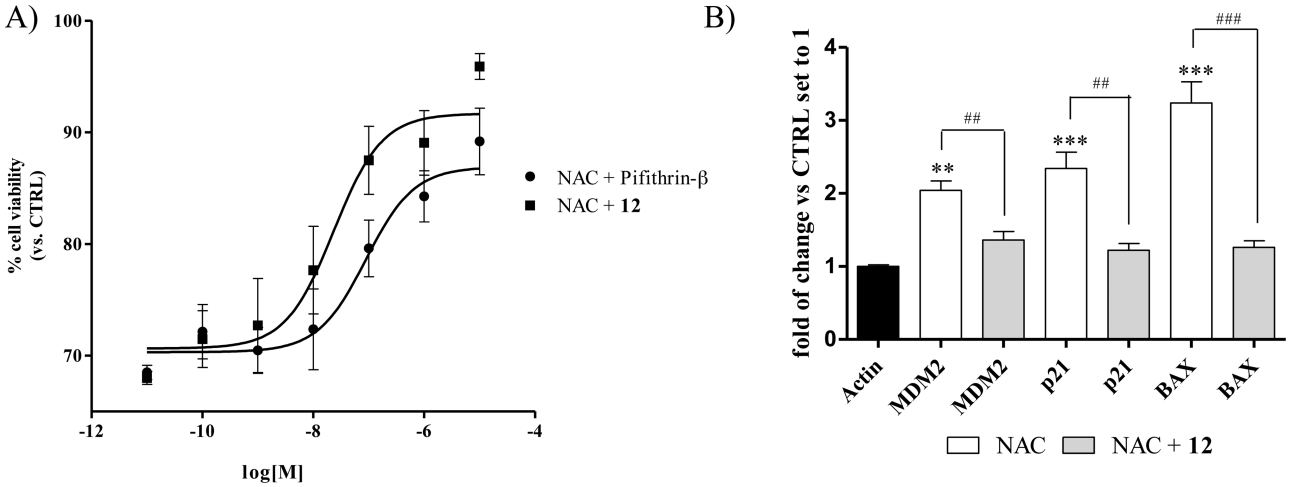

Figure 8. (A) Concentration−response curves of compound **12** and pifithrin-β. SH-SY5Y cells were treated with different concentrations of **12** (1 nM to 10 μM) in the presence of 10 μM fibrillar NAC. The data are expressed as the percentages of cell viability vs the control, which was set to 100%. Values represent the means ± SEM of at least two independent experiments. (B) Pretreatment with compound **12** preserved the increase in the mRNA levels of p53 target genes. The relative quantification of MDM2, p21, and BAX mRNA was performed by real-time PCR. SH-SY5Y cells were treated for 24 h with 10 μM fibrillar NAC in the absence or presence of 10 μM compound **12**. The data are expressed as the mRNA fold increases vs the control, which was set to 1. Values represent the means ± SEM of at least three independent experiments. $^{**}p < 0.01$ and $^{***}p < 0.001$ vs the control; $^{\#\#}p < 0.01$ and $^{\#\#\#}p < 0.001$ for NAC and **12** vs NAC.

for the better neuroprotective activity with respect to pifithrin-β.

In conclusion, the results of our study demonstrate that the AD plaque peptide fibrillar NAC activates the p53 functions in the human neuroblastoma SH-SY5Y cell line, as revealed by the increase in the levels of p53 target gene transcription, inhibition of cell growth, and induction of apoptosis; such NAC-induced cellular effects are counteracted by pifithrin-β. It is likely that NAC, like β-amyloid, may act through different types of cytotoxic mechanisms, both extracellular and intracellular, all concurrent in the activation of p53. These findings indicate that the *in vitro* NAC model could be a good predictive test for the evaluation of p53 interfering compounds as potential anti-AD agents.

Furthermore, 20 heterocyclic compounds (**3**−**22**) structurally related to pifithrin-β, but chemically different from it, were identified by screening the ZINC database using a pharmacophore-based approach. Fourteen compounds, provided with sufficient buffer solubility, were assessed for their cell safety profile in human SH-SY5Y cells. The noncytotoxic compounds (**4**, **12**, and **19**) were tested to determine if they could protect SH-SY5Y cells against fibrillar NAC. In particular, **12** turned out to be the best compound in terms of neuroprotection and cell safety, inhibiting NAC-induced cell death nearly 4 times more efficiently (EC_{50} value of 23.4 nM) than pifithrin-β (EC_{50} value of 89.1 nM), probably as a result of a more effective functional inhibition of p53 target gene transcription. Undoubtedly, a cellular model does not account for all the multiple variables of a living system, and a number of further studies have to be conducted before advocating the use of a compound as an anti-AD agent. However, given all the limitations described above, the excellent pharmacological properties, the aqueous solubility, and the druglike properties of **12** make this compound a promising lead structure for the further development of anti-AD agents.

METHODS

Materials. NAC peptide was purchased from RayBiotech, Inc. (Norcross, GA). The *in vitro* toxicology Neutral Red Assay kit and the primers used for RT-PCR (MDM2, p21, BAX, and β-actin) were obtained from Sigma (St. Louis, MO). The RNeasy Mini Kit was purchased from Qiagen S.p.A. The Script cDNA synthesis kit was furnished by Biorad s.r.l. Fluocycle II SYBR was obtained from Euroclone s.p.a. Muse Cell Cycle reagent was obtained from Millipore. Pifithrin-β and the selected heterocyclic compounds were obtained from Ambinter c/o Greenpharma (Orléans, France). All other chemicals or materials were purchased from standard sources.

Cell Model Characterization. *Preparation of the Soluble NAC Peptide.* NAC was dissolved in PBS [9.1 mM NaH_2PO_4, 1.7 mM Na_2HPO_4, and 150 mM NaCl (pH 7.4)] at a concentration of 100 μM, according to the data sheet. Gentle shaking at room temperature for 1 h or 8 days was performed to create the two aggregation states of the NAC peptide, the nonaggregated (1 h, protofibrils) and aggregated (8 days, fibrils) states. To prevent bacterial infection, the solutions were filtered and then ultrasonicated daily, as previously reported.[30]

Cell Culture. This study was conducted using the human neuroblastoma SH-SY5Y cell line, as previously reported in AD studies.[16] Cells were maintained in DMEM/F12 medium, supplemented with 15% fetal bovine serum (FBS), 1% nonessential amino acids, 2 mM L-glutamine (cell complete medium), and penicillin/streptomycin in a humidified atmosphere (5% CO_2) at 37 °C. For the experiments, confluent cells were subcultured into 100 mm^2 dishes or 96-well plates. Each well was covered with 100 μL of complete medium containing 5×10^3 cells. After 24 h, cell cultures achieved 60−70% confluence; then the cells were incubated in serum-reduced medium (2% FBS) and exposed to NAC and/or compounds for 24 h.

Cytotoxicity Assay. The NAC cytotoxicity was assessed by means of the Neutral Red Assay. This assay is based on the accumulation of the neutral red dye in the lysosomes of viable uninjured cells.[39] Briefly, NAC-treated cells were incubated for 1 h with 100 μL of neutral red dye (33 μg/mL) dissolved in serum free medium. At the end of the incubation period, cells were washed twice with the warm osmotically balanced saline solution PBS. The wash solution was removed, and the cell-incorporated dye was solubilized in 100 μL of Neutral Red Assay Solubilization Solution (50% EtOH and 1% AcOH). The cultures were allowed to stand for 10 min at room temperature while being gently stirred, to enhance the mixing of the solubilized dye. The absorbance was measured at a wavelength of 540 nm with a microplate

dx.doi.org/10.1021/cn4002208 | *ACS Chem. Neurosci.* 2014, 5, 390−399

reader. The background absorbance of multiwell plates at 690 nm was subtracted from the measurement at 540 nm. Each experiment was repeated five times.

Real-Time Quantitative RT-PCR. Gene expression was assessed by reverse transcription polymerase chain reaction (RT-PCR) as previously described.[40] In brief, total RNA was extracted from the control and cells treated with 10 μM NAC or cells pretreated with 10 μM pifithrin-β for 3 h and then supplemented with 10 μM NAC, using the RNeasy Mini Kit according to the manufacturer's instructions. The purity of the RNA samples was determined by measuring the absorbance at 260−280 nm. Reverse transcription was performed with 500 ng of total RNA using the i-Script cDNA synthesis kit following the manufacturer's instructions. The primers used for real time RT-PCR were designed to span intron−exon boundaries to ensure that products did not include genomic DNA (Table 2). The real time RT-

Table 2. Primers Used for Real-Time RT-PCR

gene	primer nucleotide sequences	product size (bp)
MDM2	forward, 5′-TCTAGGAGATTTGTTTGGCGT-3′	125
	reverse, 5′-TCACAGATGTACCTGAGTCC-3′	
p21	forward, 5′-TGCCGAAGTCAGTTCCTTG-3′	134
	reverse, 5′-CATGGGTTCTGACGGACATC-3′	
BAX	forward, 5′-TTTGCTTCAGGGTTTCATCC-3′	245
	reverse, 5′-CAGTTGAAGTTGCCGTCAGA-3′	
β-actin	forward, 5′-GCACTCTTCCAGCCTTCCTTCC-3′	254
	reverse, 5′-GAGCCGCCGATCCACACG-3′	

PCR mixtures consisted of 25 μL of Fluocycle II SYBR, 1.5 μL of both the forward and reverse primers (at a concentration of 10 μM), 3 μL of cDNA, and 19 μL of water. All reactions were performed for 40 cycles using the following temperature profiles: 98 °C for 30 s (initial denaturation), 55 °C for 30 s (annealing), and 72 °C for 3 s (extension). β-Actin was used as the housekeeping gene. PCR specificity was determined using both melting curve analysis and gel electrophoresis, and the data were analyzed by the standard curve method. mRNA levels for each sample were normalized against β-actin mRNA levels, and the relative level of expression was calculated using the C_t value.

Cell Cycle Analysis. The measurement of the percentage of cells in the G0/G1, S, and G2/M phases of the cell cycle was performed using the Muse Cell Analyzer, as previously reported.[40] Briefly, cells were treated with DMSO, 10 μM NAC, or 10 μM pifithrin-β; in parallel, cells were pre-exposed to 10 μM pifithrin-β for 3 h and then supplemented with 10 μM NAC. After 24 h, adherent cells were collected and centrifuged at 300*g* for 5 min. After being washed with 1× PBS, suspended cells were fixed and, after the slow addition of 1 mL of ice-cold 70% ethanol, maintained overnight at −20 °C. Then, a cell suspension aliquot (containing at least 2 × 10^5 cells) was centrifuged at 300*g* for 5 min, washed once with 1× PBS, and suspended in the fluorescent reagent (Muse Cell Cycle reagent). After incubation for 30 min at room temperature, in the dark, the measurements of the percentages of cells in the phases of the cell cycle were acquired.

Cell Death Assay. The living state of 24 h drug-treated cells was assessed by the MUSE cell analyzer, using specific potentiometric fluorescent dyes, as previously reported.[40] Briefly, for the cell death assay, Annexin V and propidium iodide (PI) were used as fluorescent probes. Annexin V is commonly used to detect cells expressing phosphatidylserine on the cell surface, which occurs during apoptosis; on the other hand, PI does not pass through intact cell membranes, so it is considered as a marker of necrotic death. We simultaneously measured the level of expression of phosphatidylserine on the cell surface and cellular plasma membrane permeabilization (using the Muse annexin and cell death assay). Briefly, cells were treated for 24 h with DMSO, 10 μM NAC, or 10 μM pifithrin-β; in parallel, cells were pre-exposed to 10 μM pifithrin-β for 3 h and then supplemented with 10 μM NAC for 24 h. After being exposed to the drug, both floating and adherent cells were collected, centrifuged at 300*g* for 5 min, and suspended in cell culture medium. Then, a 100 μL aliquot of a cell suspension (~5 × 10^4 cells/mL) was added to 100 μL of fluorescent reagent and the mixture incubated for 10 min at room temperature. After the incubation period, the percentages of living, apoptotic, and dead cells were acquired and analyzed, by the Muse Cell Analyzer in accordance with the Millipore guidelines.

Virtual Screening. *Pharmacophore Hypothesis Generation.* With compound **2** as a starting point,[22] pharmacophoric features were automatically generated with phase (Phase, version 3.3) using the default set of six chemical features: hydrogen bond acceptor (A), hydrogen bond donor (D), hydrophobic group (H), negatively charged group (N), positively charged group (P), and aromatic ring (R). Because the template ligand was highly rigid, only one hypothesis was produced; this contained four aromatic rings, a hydrogen bond acceptor, and a hydrophobic group (see Figure 5).

Database Preparation. The commercial chemical database ZINC "Leads Now", containing more than 1983960 compounds, was processed through redundancy checking and Lipinski filters to select compounds provided with better druglike properties. Database molecules were prepared using LigPrep (LigPrep, version 2.5, Schrödinger, LLC) with Epik (Epik, version 2.2, Schrödinger, LLC). Conformational sampling was performed on all database molecules using the ConfGen search algorithm (ConfGen, version 2.3, Schrödinger, LLC). Using Phase,[41] the database was indexed with the automatic creation of pharmacophoric sites for each conformer to allow rapid database alignments and screening.

Pharmacophore-Based Database Screening. Screening molecules were required to match a minimum of four out of six sites. The distance matching tolerance was set to 2.0 Å as a balance between stringent and loose-fitting matching alignment. Database hits were ranked in order of their fitness score[41] as a measure of how well the aligned conformer matches the hypothesis based on root-mean-square deviation site matching, vector alignments, and volume terms. The fitness scoring function is an equally weighted composite of these three terms and ranges from 0 to 3, as implemented in the default database screening in Phase. In our virtual screening campaign, only those compounds possessing a fitness score of >2 (187 compounds) were considered for further analysis. These compounds were first clustered into chemically homogeneous groups and then visually inspected. Eventually, we selected the 20 compounds listed in Table 1 that were purchased to be biologically evaluated.

^{1}H NMR and Elemental Analyses. The structures of the purchased compounds was confirmed by ^{1}H NMR spectra and elemental analysis. Routine nuclear magnetic resonance spectra were recorded in a DMSO-d_6 solution on a Varian Gemini 200 spectrometer operating at 200 MHz. Combustion analyses on tested compounds were performed by our analytical laboratory in Pisa. All compounds were ≥95% pure.

Assessment of Compound Solubility in Cell Experimental Buffer. The solubility of each compound under the experimental conditions (cell culturing complete medium with 1% DMSO) was estimated as previously reported.[39] One micromole of each compound was added first with DMSO (100 μL) and then with cell complete medium (9.9 mL). The mixture was shaken at room temperature for 10 min and then visually inspected. The completely solubilized compounds were considered testable molecules. Incompletely solubilized compounds were also shaken at 37 °C for 30 min. The compounds were classified as nontestable compounds if their insoluble parts could be visually detected after this prolonged shaking.

Neuroprotective Activity of Selected Compounds. Cytotoxicity and Neuroprotection Assays. The cytotoxicity of the investigated compounds (1 and 10 μM) was assessed by means of the Neutral Red Assay, as previously reported for NAC-exposed cells. The assessment of compound neuroprotective effects was performed by pre-exposing the cells to pifithrin-β and the tested compound (1 and 10 μM) for 3 h. Then, 10 μM fibrillar NAC was added to cells and the mixture incubated for 24 h. The viability was assessed using the Neutral Red Assay as described above.

EC_{50} Determination. Cells were pretreated with seven different concentrations of pifithrin-β (1 nM to 10 μM) or compound **12** (1

dx.doi.org/10.1021/cn4002208 | ACS Chem. Neurosci. 2014, 5, 390−399

nM to 10 μM) for 3 h. After this, 10 μM fibrillar NAC was added to cells and the mixture incubated for 24 h. The viability was assessed using the Neutral Red Assay as described above. The concentrations (EC_{50}) of compound **12** and pifithrin-β that could inhibit NAC-induced cell death by 50% were evaluated by nonlinear regression fitting of the data to a one-site model. Pseudo-Hill slopes were calculated by a nonlinear regression fit of the data to a sigmoidal concentration−response equation (variable slope):

$$\%\ \text{viability} = \text{minimal}\ \%\ \text{viability} + \frac{(\text{maximal}\ \%\ \text{viability} - \text{minimal}\ \%\ \text{viability})}{[1 + 10(\log EC_{50} - X)^n]}$$

where X is the logarithm of the inhibitor concentration and n is the pseudo-Hill slope. The maximal % viability and minimal % viability were experimentally determined after NAC exposure and compound treatment. EC_{50} values and 95% confidence intervals (CIs) were derived from the sigmoid fits to the percent control transformed data shown using GraphPad Prism version 5.0 (GraphPad Software, San Diego, CA).

Data Analysis. For data analysis and graphic presentations, the nonlinear multipurpose curve-fitting program Graph-Pad Prism version 5 was used. All data are presented as means ± SEM. Statistical analyses were performed by one-way analysis of variance (with the post hoc Bonferroni test). $p < 0.05$ was considered statistically significant.

■ ASSOCIATED CONTENT

Supporting Information

IUPAC nomenclature, structural formulas, and ^{1}H NMR data of heterocyclic compounds **1**−**22** (Table S1) and analytical data (combustion analysis) of compounds **1**−**22** (Table S2). This material is available free of charge via the Internet at http://pubs.acs.org.

■ AUTHOR INFORMATION

Corresponding Author

*Dipartimento di Farmacia, Università di Pisa, via Bonanno Pisano 6, 56126 Pisa, Italy. Phone: +390502219509/522. Fax: +390502219608/9. E-mail: claudia.martini@unipi.it.

Author Contributions

C.M., E.N., and G.G. conceived the project. E.D.P. performed the cell death assay and EC_{50} determination assays, analyzed all biological data, and wrote the manuscript. V.L.P. performed the pharmacophore hypothesis generation, database preparation, and pharmacophore database screening. E.D.P. and V.L.P. contributed equally to this work. C.G. prepared the NAC and performed cell culturing, real-time RT-PCR, cell cycle analysis, and cytotoxicity and neuroprotection assays. L.M. performed the virtual screening analysis. B.C. and S.T. performed the ^{1}H NMR and elemental analyses and revised the manuscript. F.D.S. revised the manuscript. G.G. and C.M. wrote and revised the manuscript.

Funding

The Italian Ministry of Education, University and Research (MIUR, Italy; PRIN 2009 Project, to G.G.) and the University of Pisa financially supported this work.

Notes

The authors declare no competing financial interest.

■ ABBREVIATIONS

AD, Alzheimer's disease; NAC, non-β-amyloid component; IBT, imidazo[2,1-*b*]benzothiazole; PI, propidium iodide; SEM, standard error of the mean; RT-PCR, reverse transcription polymerase chain reaction.

■ REFERENCES

(1) Nordberg, A. (1992) Neuroreceptor changes in Alzheimer disease. *Cerebrovascular and Brain Metabolism Reviews 4*, 303−328.
(2) Citron, M. (2010) Alzheimer's disease: Strategies for disease modification. *Nat. Rev. Drug Discovery 9*, 387−398.
(3) Kitamura, Y., Shimohama, S., Kamoshima, W., Matsuoka, Y., Nomura, Y., and Taniguchi, T. (1997) Changes of p53 in the brains of patients with Alzheimer's disease. *Biochem. Biophys. Res. Commun. 232*, 418−421.
(4) de la Monte, S. M., Sohn, Y. K., and Wands, J. R. (1997) Correlates of p53 and Fas (CD95)-mediated apoptosis in Alzheimer's disease. *J. Neurol. Sci. 152*, 73−83.
(5) Levine, A. J. (1997) P53, the cellular gatekeeper for growth and division. *Cell 88*, 323−331.
(6) Lemasters, J. J., Nieminen, A. L., Qian, T., Trost, L. C., Elmore, S. P., Nishimura, Y., Crowe, R. A., Cascio, W. E., Bradham, C. A., Brenner, D. A., and Herman, B. (1998) The mitochondrial permeability transition in cell death: A common mechanism in necrosis, apoptosis and autophagy. *Biochim. Biophys. Acta 10*, 177−196.
(7) Zhang, Y., McLaughlin, R., Goodyer, C., and LeBlanc, A. (2002) Selective cytotoxicity of intracellular amyloid β peptide1−42 through p53 and Bax in cultured primary human neurons. *J. Cell Biol. 156*, 519−529.
(8) Davenport, C. M., Sevastou, I. G., Hooper, C., and Pocock, J. (2010) Inhibiting p53 pathways in microglia attenuates microglial-evoked neurotoxicity following exposure to Alzheimer peptides. *J. Neurochem. 112*, 552−563.
(9) LaFerla, F. M., Hall, C. K., Ngo, L., and Jay, G. (1996) Extracellular deposition of β-amyloid upon p53-dependent neuronal cell death in transgenic mice. *J. Clin. Invest. 98*, 1626−1632.
(10) Ueda, K., Fukushima, H., Masliah, E., Xia, Y., Iwai, A., Otero, D., Kondo, J., Ihara, Y., and Saitoh, T. (1993) Molecular cloning of a novel component of amyloid in Alzheimer's disease. *Proc. Natl. Acad. Sci. U.S.A. 90*, 11282−11286.
(11) Iwai, A., Masliah, E., Yoshimoto, M., De Silva, R., Ge, N., Kittel, A., and Saitoh, T. (1994) The precursor protein of non-Aβ component of Alzheimer's disease amyloid (NACP) is a presynaptic protein of the central nervous system. *Neuron 14*, 467−475.
(12) Masliah, E., Iwai, A., Mallory, M., Uéda, K., and Saitoh, T. (1996) Altered presynaptic protein NACP is associated with plaque formation and neurodegeneration in Alzheimer's disease. *Am. J. Pathol. 148*, 201−210.
(13) El-Agnaf, O. M., Jakes, R., Curran, M. D., Middleton, D., Ingenito, R., Bianchi, E., Pessi, A., Neill, D., and Wallace, A. (1998) Aggregates from mutant and wild-type α-synuclein proteins and NAC peptide induce apoptotic cell death in human neuroblastoma cells by formation of β-sheet and amyloid-like filaments. *FEBS Lett. 440*, 71−75.
(14) Bodles, A. M., Guthrie, D. J., Harriott, P., Campbell, P., and Irvine, G. B. (2000) Toxicity of non-Aβ component of Alzheimer's disease amyloid, and N-terminal fragments thereof, correlates to formation of β-sheet structure and fibrils. *Eur. J. Biochem. 267*, 2186−2194.
(15) Kaźmierczak, A., Czapski, G. A., Adamczyk, A., Gajkowska, B., and Strosznajder, J. B. (2011) A novel mechanism of non-Aβ component of Alzheimer's disease amyloid (NAC) neurotoxicity. Interplay between p53 protein and cyclin-dependent kinase 5 (Cdk5). *Neurochem. Int. 58*, 206−214.
(16) Komarov, P. G., Komarova, E. A., Kondratov, R. V., Christov-Tselkov, K., Coon, J. S., Chernov, M. V., and Gudkov, A. V. (1999) A chemical inhibitor of p53 that protects mice from the side effects of cancer therapy. *Science 285*, 1733−1737.
(17) Culmsee, C., Zhu, X., Yu, Q. S., Chan, S. L., Camandola, S., Guo, Z., Greig, N. H., and Mattson, M. P. (2001) A synthetic inhibitor

of p53 protects neurons against death induced by ischemic and excitotoxic insults, and amyloid β-peptide. *J. Neurochem. 77*, 220−228.
(18) Leker, R. R., Aharonowiz, M., Greig, N. H., and Ovadia, H. (2004) The role of p53-induced apoptosis in cerebral ischemia: Effects of the p53 inhibitor pifithrin α. *Exp. Neurol. 187*, 478−486.
(19) Zhu, X., Yu, Q. S., Cutler, R. G., Culmsee, C. W., Holloway, H. W., Lahiri, D. K., Mattson, M. P., and Greig, N. H. (2002) Novel p53 inactivators with neuroprotective action: Syntheses and pharmacological evaluation of 2-imino-2,3,4,5,6,7-hexahydrobenzothiazole and 2-imino-2,3,4,5,6,7-hexahydrobenzoxazole derivatives. *J. Med. Chem. 45*, 5090−5097.
(20) Pietrancosta, N., Moumen, A., Dono, R., Lingor, P., Planchamp, V., Lamballe, F., Bahr, M., Kraus, J.-L., and Maina, F. (2006) Iminotetrahydro-benzothiazole derivatives as p53 Inhibitors: Discovery of a highly potent in vivo inhibitor and its action mechanism. *J. Med. Chem. 49*, 3645−3652.
(21) Pietrancosta, N., Maina, F., Dono, R., Moumen, A., Garino, C., Laras, Y., Burlet, S., Quelever, G., and Kraus, J.-L. (2005) Novel cyclised pifithrin-α p53 inactivators: Synthesis and biological studies. *Bioorg. Med. Chem. Lett. 15*, 1561−1564.
(22) Barchechath, S. D., Tawatao, R. I., Corr, M., Carson, D. A., and Cottam, H. B. (2005) Inhibitors of apoptosis in lymphocytes: Synthesis and biological evaluation of compounds related to pifithrin-alpha. *J. Med. Chem. 48*, 6409−6422.
(23) Christodoulou, M. S., Colombo, F., Passarella, D., Ieronimo, G., Zuco, V., De Cesare, M., and Zunino, F. (2011) Synthesis and biological evaluation of imidazolo[2,1-*b*]benzothiazole derivatives, as potential p53 inhibitors. *Bioorg. Med. Chem. 19*, 1649−1657.
(24) Simoni, E., Daniele, S., Bottegoni, G., Pizzirani, D., Trincavelli, M. L., Goldoni, L., Tarozzo, G., Reggiani, A., Martini, C., Piomelli, D., Melchiorre, C., Rosini, M., and Cavalli, A. (2012) Combining galantamine and memantine in multitargeted, new chemical entities potentially useful in Alzheimer's disease. *J. Med. Chem. 55*, 9708−9721.
(25) Gilbert, B. J. (2013) The role of amyloid β in the pathogenesis of Alzheimer's disease. *J. Clin. Pathol. 66*, 362−366.
(26) Kayed, R., Head, E., Thompson, J. L., McIntire, T. M., Milton, S. C., Cotman, C. W., and Glabe, C. G. (2003) Common structure of soluble amyloid oligomers implies common mechanism of pathogenesis. *Science 300*, 486−489.
(27) Tamagno, E., Bardini, P., Guglielmotto, M., Danni, O., and Tabaton, M. (2006) The various aggregation states of β-amyloid 1−42 mediate different effects on oxidative stress, neurodegeneration, and BACE-1 expression. *Free Radical Biol. Med. 41*, 202−212.
(28) Du, H. N., Tang, L., Luo, X. Y., Li, H. T., Hu, J., Zhou, J. W., and Hu, H. Y. (2003) A peptide motif consisting of glycine, alanine, and valine is required for the fibrillization and cytotoxicity of human α-synuclein. *Biochemistry 42*, 8870−8878.
(29) Adamczyk, A., Jeśko, H., and Strosznajder, R. P. (2005) Alzheimer's disease related peptides affected cholinergic receptor mediated poly(ADP-ribose) polymerase activity in the hippocampus. *Folia Neuropathol. 43*, 139−142.
(30) Hunya, A., Földi, I., Szegedi, V., Soós, K., Zarándi, M., Szabó, A., Zádori, D., Penke, B., and Datki, Z. L. (2008) Differences between normal and α-synuclein overexpressing SH-SY5Y neuroblastoma cells after Aβ(1−42) and NAC treatment. *Brain Res. Bull. 75*, 648−654.
(31) Kim, E. M., Elliot, J. J., Hobson, P., and O'Hare, E. (2009) Effects of intrahippocampal NAC 61−95 injections on memory in the rat and attenuation with vitamin E. *Progress in Neuro-psychopharmacology & Biological Psychiatry 33*, 945−951.
(32) O'Hare, E., Elliott, J. J., Hobson, P., O'Mara, S. M., Spanswick, D., and Kim, E. M. (2010) Bilateral intrahippocampal NAC61−95 effects on behavior and moderation with L-NAME treatment. *Neurosci. Res. 66*, 213−218.
(33) O'Hare, E., Elliott, J. J., Hobson, P., Spanswick, D., and Kim, E. M. (2010) Behavioural deterioration induced by intrahippocampal NAC61−95 injections and attenuation with ibuprofen. *Behav. Brain Res. 208*, 274−277.
(34) Vogelstein, B., Lane, D., and Levine, A. J. (2000) Surfing the p53 network. *Nature 408*, 307−310.
(35) Martin, Y. C. (1992) 3D Database searching. *J. Med. Chem. 35*, 2145−2154.
(36) Irwin, J. J., and Shoichet, B. K. (2005) ZINC: A free database of commercially available compounds for virtual screening. *J. Chem. Inf. Model. 45*, 177−182.
(37) Primofiore, G., Da Settimo, F., Taliani, S., Marini, A. M., La Motta, C., Novellino, E., Greco, G., Gesi, M., Trincavelli, L., and Martini, C. (2000) 3-Aryl-[1,2,4]triazino[4,3-*a*]benzimidazol-4(10*H*)-ones: Tricyclic heteroaromatic derivatives as a new class of benzodiazepine receptor ligands. *J. Med. Chem. 43*, 96−102.
(38) Balakin, K., Ivanenkov, Y. A., Skorenko, A. V., Nikolsky, Y. V., Savchuk, N. P., and Ivashchenko, A. A. (2004) In Silico Estimation of DMSO Solubility of Organic Compounds for Bioscreening. *J. Biomol. Screening 9*, 22−31.
(39) Borenfreund, E., and Puerner, J. (1985) Toxicity determined in vitro by morphological alterations and neutral red absorption. *Toxicol. Lett. 24*, 119−124.
(40) Costa, B., Bendinelli, S., Gabelloni, P., Da Pozzo, E., Daniele, S., Scatena, F., Vanacore, R., Campiglia, P., Bertamino, A., Gomez-Monterrey, I., Sorriento, D., Del Giudice, C., Iaccarino, G., Novellino, E., and Martini, C. (2013) Human Glioblastoma Multiforme: p53 Reactivation by a Novel MDM2 Inhibitor. *PLoS One 8*, e72281.
(41) Dixon, S. L., Smondyrev, A. M., and Rao, S. N. (2006) PHASE: A novel approach to pharmacophore modeling and 3D database searching. *Chem. Biol. Drug Des. 67*, 370−372.